Research Article

Development of Screw-Based 3D Printing Machine and Process Experiments for Short Fiber Reinforced Polymer Composites

Thanapat Sangkharat* and Laongdaw Techawinyutham
Department of Production and Robotics Engineering, Faculty of Engineering, King Mongkut's University of Technology North Bangkok, Bangkok, Thailand

* Corresponding author. E-mail: thanapat.s@eng.kmutnb.ac.th DOI: 10.14416/j.asep.2023.11.005
Received: 8 July 2023; Revised: 14 August 2023; Accepted: 21 September 2023; Published online: 14 November 2023

Abstract
3D printing is one of the flexible additive manufacturing (AM) processes that can be used to fabricate parts from various types of materials such as polymers, metal, and ceramic. 3D printing process is one of the famous techniques for printing the product from the filament causing material degradation. Granule-based 3D printing or screw-based material extrusion 3D printing is an alternative process that can create the parts from plastic or composite granule raw materials. However, there are limited use and study in the designation of granule-based 3D printing and process parameters including material temperature, heat bed temperature, nozzle size, and printing speed. These process parameters play a significant role in the properties of 3D printing parts. Some parameters cannot be adjusted in the commercial 3D printing process. Thus, the purposes of this study are to develop a screw-based material extrusion 3D printing machine that can freely adjust the process parameters and to investigate the effect of 3D printing parameters on the appearance and mechanical properties of printed parts. Pellets of neat acrylonitrile butadiene styrene (ABS) and short glass fiber/ABS composites are used in the experiments. Six process parameters were studied, including % fiberglass, printing temperature, printing speed, nozzle size, % Infill, and heat bed temperature. Each parameter has 3 levels, which were designed by the Taguchi L18 method. The results were evaluated by the main effect plot method and showed that the printing speed, nozzle size, and %fiberglass are the top 3 parameters that affect tensile strength. The nozzle size, %infill, and %fiberglass are the top 3 parameters that affect Young's modulus. The granule-based 3D printing machine was completely developed; however, the extruded plastic line from the nozzle was difficult to control resulting in poor product quality. Thus, the feedback control for controlling the screw-extruder speed and temperature will be developed in future work.

Keywords: Short fiberglass reinforced, Granule-based 3D printer, Screw-based material extrusion, Additive manufacturing, Composite materials

1 Introduction

The machining process of removing unnecessary material from the raw part is the conventional process which makes a lot of materials waste [1]. Therefore, the additive manufacturing (AM) process is widely used to replace the conventional process, which uses the layer-by-layer concept for fabricating the product making less waste of materials [2]. 3D printing is one of the AM processes that is widely used in many sectors [3], [4]. It is applied in factories, medical [5]–[7], aerospace [8], etc. In addition, AM can fabricate parts from various materials, such as polymer, composite, metal, and ceramic. For this reason, AM is an interesting manufacturing process [9], [10]. Material extrusion (MEX) or fused filament fabrication (FFF) is one of the 3D printing processes, which the melted material is printed layer-by-layer to build the product. The first FFF process was presented by Crump in 1988, which used basic concepts to fabricate complex products

called "melted extrusion AM process". The FFF machine includes a filament feeding, a heater, a nozzle, and a 3-axis movement machine.

Various low melting temperatures thermoplastics such as ABS, polylactic acid (PLA), polyethylene terephthalate (PET), polypropylene (PP), thermoplastic polyurethane (TPU), and polyamide (PA) can be fabricated in complex shapes by FFF process, which can reduce the usage of complex equipment or mold [11]. However, the products from the FFF process consist of porosity and have low mechanical properties [12]. For this reason, the FFF process is used for fabricating the prototype more than forming a product for applications [13]. Many studies are trying to improve the FFF process by developing printing machines and materials. Choi *et al.*, [14] developed the FFF machine and located the nozzle under the moving platform. This machine can print on any freeform surface, so it can be used for repairing and expanding the product. Mireles *et al.*, [15] developed the print head and modified the printing tool path; moreover, they printed the low melting temperature metal using an FFF machine. Lee *et al.*, [16] developed the rapid prototype by cooperating with FFF and a 5-axis milling machine, which can improve the flexibility for manufacturing the product. In addition, this machine can immediately finish the product's surface after the 3D printing process. Maidin *et al.*, [17] improved the hardness of FFF products by using vacuum assisted system. The system can sustain heat for bonding between layers which can improve the workpiece strength. Therefore, the vacuum for reducing the staircase effect of the product from the FFF process was used [18]. Sorina-Heras *et al.*, [19] presented a real time system for detecting filament abnormalities, which was used for the FFF machine. They developed an abnormal filament detection system by using the mechanical system and cooperation with an optical encoder. This system can detect abnormal filaments. It can protect the print head from wear and damage. Al-Ahmari *et al.*, [20] developed the print orientation optimization system. The purpose of the system was to reduce the waste of material from support and the printing time; moreover, this system can make good quality products. Furthermore, the development of 3D printing machines can improve product quality. The 3D printing process parameters and composite materials were interesting to study their influence on product quality [21]. Dogru *et al.*, [22] studied the effect of aging and infill patterns on mechanical properties. They reported parallel printing to tensile direction got a lower tensile strength than cross printing. Abeykoon [23] studied the mechanical properties of various materials, such as PLA, ABS, CFR PLA, CFR ABS, and CNT ABS. They studied the effect of infill density, infill speed, infill pattern, and printing temperature on the product strength. It was found that Young's modulus increased when the infill density and printing temperature were increased. Kamaal [24] studied the tensile and impact strength of composite carbon fiber and PLA. They modified the build direction, infill percentage, and layer height. The results showed that the tensile strength increased when increased the infill percentage and layer height. The impact strength increased when the infill percentage was increased, and layer height was decreased. Omer [25] performed experiments to determine the effects of layer thickness, layer position, and infill percentage on tensile strength. The composite material of short fiber and PLA were used in the experiment. They reported that an increase in layer thickness and infill percentage improved the tensile strength. Moreover, Artificial Neural Network (ANN) was developed for the prediction and optimization of the tensile strength. V. Durga Prasada Rao [26] discussed the effect of print temperature, layer thickness, and infill pattern on the PLA printing workpiece. They found that an increase in the printing temperature from 205–225 °C can enhance the tensile strength. Besides composite materials that can be used to fabricate industrial parts, they can be applied in medical applications, such as biosensors and biomaterials [27]–[30]. Thus, the composited composite material is still an interesting research issue.

In this study, the granule-based 3D printing machine was developed consisting of a screw feeder and a 3-axis machine to print ABS and glass fiber/ABS composites. The granule-based 3D printing machine was used to study the effect of process parameters on the mechanical properties of workpieces. The studied process parameters are % fiberglass, printing temperature, printing speed, nozzle size, % infill, and heat bed temperature.

2 Materials and Methods

2.1 *3D printing machine*

This study developed the granule-based 3D printing

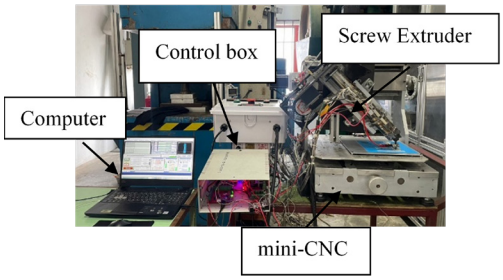

Figure 1: Overview of the 3D printing machine.

machine by using a screw-based extrusion machine. The machine was used to print dog-bone specimens for the tensile test. Due to the limitation of commercial 3D printers for adjusting the printing parameters, the screw-based material extrusion machine was built. The machine was a collaboration of polymer screw extrusion and 3 axis CNC machine. The machine was controlled by a control box and computer.

The single screw extruder was used. The outside diameter and inside diameter of the screw cylinder were 40 mm and 30 mm, respectively. The 4 sets of heaters and temperature sensors were installed outside of the cylinder. The heater set 1 to set 3 were clamped on the cylinder and the last set was located at the nozzle as shown in Figure 1. All the heater sets can adjust the heating temperature via the control box.

The stepping motor was located at the end of the screw extruder for rotating the screw extruder. The rotating speed of the motor can be adjusted ranging from 0–60 Rev per min. The 3-axis mini-CNC was used for moving the nozzle to the printing position. The movement resolution of the machine was 0.1 mm on the X, Y, and Z axes. The movement positions were controlled from MACH 3 software. This software was installed on the computer and cooperated with SOLIDWORK and PRUSA software. The printing and moving parameters can be adjusted from the software.

The 3 sets of heaters and sensors were located in the extruder cylinder. The position of the first heater and sensor was 130 mm from the end of the cylinder. The second and the third heaters and sensors were 190 mm and 250 mm. The heaters were 220 VAC/350 W, K-type thermocouple temperature sensors. The measuring range was 0–350 °C. The fourth set of heater and sensor was placed at the nozzle. This heater was 12 VDC/ 40 W, and the sensor was a K-type thermocouple. Figure 2 shows the installation of heaters and sensors.

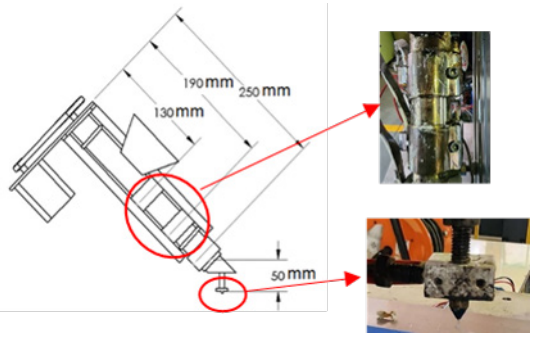

Figure 2: The installation of heaters and temperature sensors.

The ABS polymer (GA400 Polimaxx, IRPC PCL, Thailand) reinforced with short fiberglass was used in this study. The average diameter and length of glass fiber (YTD fiberglass, China) were 11 and 155 µm, respectively.

2.2 *Experiments*

The 6 process parameters were tested in this study: 1) the mixing ratio between glass fiber and ABS (% fiberglass), 2) the nozzle temperature (printing temperature), 3) the speed of the nozzle movement (printing speed), 4) the size of the nozzle (nozzle size), 5) the percentage of the material infill in the 3D printing process (% infill) and 6) the heat bed temperature. Each parameter has 3 levels. This study used Taguchi L18 to design the 18 experimental cases. The details of testing parameters in each case are shown in Tables 1 and 2.

Table 1: The process parameters were studied

Factor	Level 1	Level 2	Level 3
(A) % Fiberglass: %	0	20	25
(B) Maximum temperature for printing: °C	205	210	215
(C) Speed for print moves: mm/sec	8	12	16
(D) Nozzle size: mm.	0.3	0.4	0.5
(E) % Infill: %	90	95	100
(F) Heat bed temperature: °C	40	50	60

The glass fiber and ABS were mixed in various ratios (Table 2) by using a co-twin screw extruder. The composites were extruded and cut to the granule (Figure 3) for printing the dog-bone shape by a screw-based material extrusion machine. Then, the granule was printed to the dog-bone shape and tested the tensile

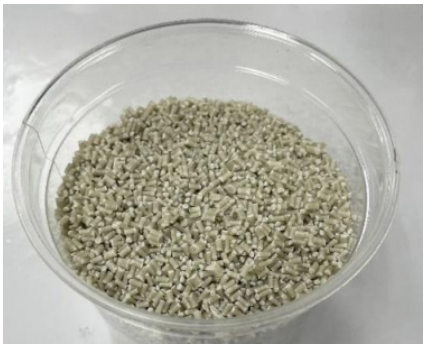

Figure 3: Granule of short glass fiber/ABS composites.

properties with a universal tensile testing machine (Cometech, QC-506M1) with a gauge length of 50 mm and tension speed of 10 mm/min. The tensile test followed the ASTM D638-14 [31]. Three experiments were performed. The tensile strength and Young's modulus were analyzed and discussed.

Table 2: Taguchi L18 design table

Case	A	B	C	D	E	F
1	0	205	8	0.3	90	40
2	0	210	12	0.4	95	50
3	0	215	16	0.5	100	60
4	20	205	8	0.4	95	60
5	20	210	12	0.5	100	40
6	20	215	16	0.3	90	50
7	25	205	12	0.3	100	50
8	25	210	16	0.4	90	60
9	25	215	8	0.5	95	40
10	0	205	16	0.5	95	50
11	0	210	8	0.3	100	60
12	0	215	12	0.4	90	40
13	20	205	12	0.5	90	60
14	20	210	16	0.3	95	40
15	20	215	8	0.4	100	50
16	25	205	16	0.4	100	40
17	25	210	8	0.5	90	50
18	25	215	12	0.3	95	60

3 Results and Discussion

3.1 *3D printing machine*

This study succeeds in developing a granule-based 3D printer as presented in Figure 1. The machine including a single screw extruder and a 3-axis min-CNC machine can print various pellet types such as PP, ABS, and fiberglass/ABS composite. Figure 3 shows the samples

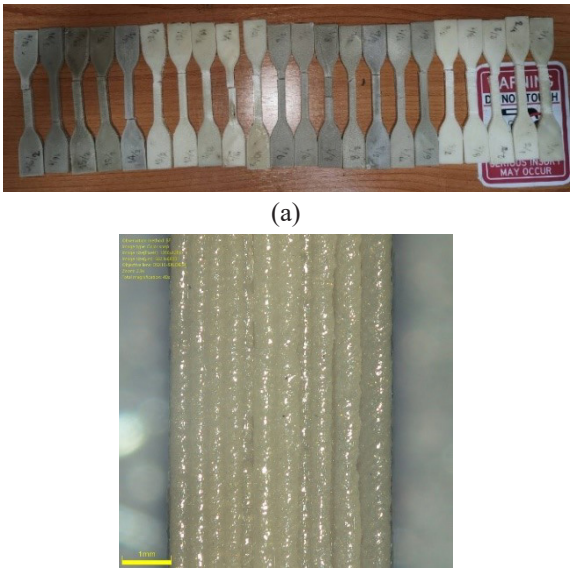

(a)

(b)

Figure 4: Photograph of (a) workpiece samples from the experiments and (b) the image from an optical microscope at 40x.

that were printed from the granule-based 3D printer. The extrusion and printing temperature can be changed by setting 4 sets of heaters and sensors. Figure 4 shows the temperature distribution in the extruder cylinder with setting heater 1 = 150 °C, heater 2 = 180 °C, heater 3 = 210 °C, and heater 4 = 210 °C. The distances in the graph are measured from the end of the extruder to the nozzle. These heating temperatures and temperature distribution were similar to the results from Kumar *et al.*, [32], [33]. Thus, the graph shows the temperatures at different positions along the extruder cylinder. The trend of temperature increases step by step. The actual temperatures of the cylinder increased nearly to the setting temperature. The temperature at heaters 1 and 2 positions are slightly lower than the setting temperature because of the transferring of temperature to plastic pellets since this position is located near the hopper.

This granule-based 3D printing machine can be used for printing various types of materials; therefore, filament preparation is unnecessary. This 3D printing machine successfully printed the specimens as shown in Figure 4(a). Figure 4(b) shows the sample image from the optical microscope with a smooth printing track and polymer line. However, the size of each layer was not equal, and it was difficult to control

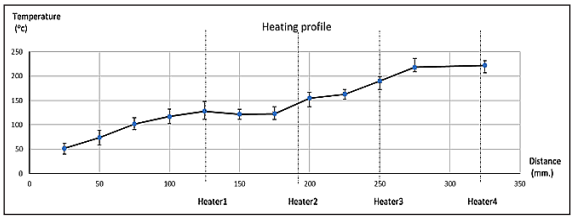

Figure 5: The temperature distribution of the extruder cylinder.

the consistency of the printed polymer line from the 3D printing extruder because many parameters influence the flow rate, pressure, and temperature in the extruder. Besides, the nozzle is small (0.3–0.5 mm.) so the variation in flow rate, pressure, and temperature played a significant effect on the consistency of the printed polymer line (Figure 5). Thus, the quality of the workpiece surface can be improved by improving the consistency of the printed polymer line.

3.2 *Taguchi method*

The 3D printing machine was used to conduct the experiments. The Taguchi method was used to design the experiment in this study as presented in Table 2. The tensile strength and Young's modulus were studied as presented in Table 3. The main effect plots were used for analyzing the results and the large-is-better signal-to-noise (SN) type was used.

Table 3: Tensile strength and Young's modulus

Case	Tensile Strength	Young's Modulus
1	38.66	1285.37
2	29.42	1201.57
3	26.78	1170.67
4	37.87	1054.02
5	26.08	1152.34
6	17.12	1073.69
7	30.57	1373.92
8	26.00	1224.22
9	22.15	1074.33
10	34.70	1125.35
11	30.57	1229.34
12	35.34	1065.50
13	21.49	975.95
14	22.32	1299.57
15	36.44	1224.22
16	29.29	1303.07
17	28.22	1104.70
18	31.20	1336.11

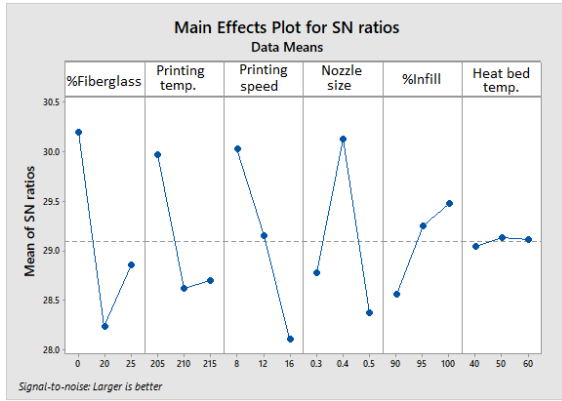

Figure 6: Main effect plot of tensile strength.

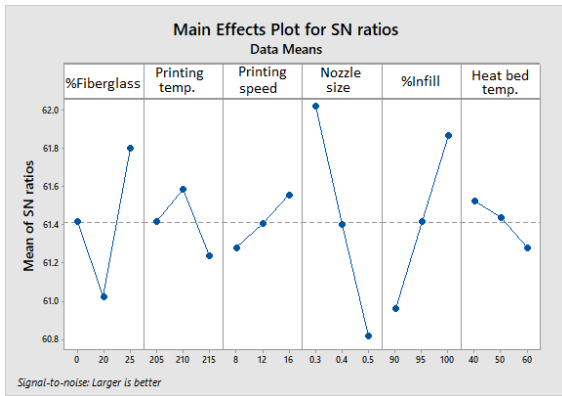

Figure 7: Main effect plot of Young's modulus.

3.2.1 Main effect plots

The main effect plots of tensile strength and Young's modulus are shown in Figures 6 and 7, respectively. The 6 process parameters are studied: 1) % fiberglass, 2) printing temperature, 3) printing speed, 4) nozzle size, 5) % infill, and 6) heat bed temperature. The printing speed, nozzle size, and %fiberglass are the top 3 parameters that show the highest effect on tensile strength. The samples with a printing speed of 8 mm/s have the highest tensile strength value of 30.03 MPa. The samples with a printing speed of 16 mm/s provide the lowest tensile strength value of 28.11 MPa since high printing speed caused high variation of extruded plastic size and small gap between layers. The samples without fiberglass presented the highest tensile strength value of 30.19 MPa. However, the samples with %fiberglass of 20 %wt showed the lowest tensile

strength value of 28.24 MPa, which was probably because of poor fiber-matrix adhesion reducing stress transferring. Corresponding to the work of Jiang *et al.*, [34], the tensile strength of short fiber-reinforced samples decreased when the load direction did not apply in the fiber direction. This study printed the sample by using an infill direction equal to 45 degrees which is not the load direction. The samples with a nozzle size of 0.4 mm had the highest tensile strength value of 30.13 MPa; however, the samples with a nozzle size of 0.5 mm provided the lowest tensile strength value of 28.38 MPa since it was probably because the large nozzle extruded a high amount of plastic which was difficult to control the consisting of extruded plastic.

The nozzle size, %infill, and %fiberglass are the top 3 parameters that affect Young's modulus as shown in Figure 7. The samples with a nozzle size of 0.3 mm had the highest Young's modulus value of 62.02 MPa; however, the samples with a nozzle size of 0.5 mm showed the minimum Young's modulus value of 60.82 MPa. The increase in nozzle size decreased Young's modulus, which was also examined in tensile strength results. The samples with %infill of 100% provided the maximum Young's modulus value of 61.87 MPa. However, the samples with nozzle %infill of 90% got the lowest Young's modulus value of 60.96 MPa. Thus, the increase in %infill slightly enhanced the Young's modulus because the specimens were completely full-filled which can support more load. The samples with %fiberglass of 25 %wt had the highest Young's modulus value of 61.80 MPa. However, the samples with %fiberglass of 20 %wt had the lowest Young's modulus value of 61.02 MPa since fiberglass improved the rigidity of its composite. The results are in the same direction as other research reported that %infill and %Fiberglass affect the strength of 3D printing parts [24]–[26], [35].

3.2.1 Interaction plot and ANOVA

An interaction plot as presented in Figure 8 presents the impact of changing one parameter value with an effect on the other parameters. In this study, the interaction plot of the top 3 parameters that show the highest effect on tensile strength (printing speed, nozzle size, and %fiberglass) and Young's modulus (nozzle size, %infill, and %fiberglass) are drawn to confirm the interaction effect. The non-parallel lines in the interaction plot of nozzle size and %fiberglass show that the effect of nozzle size on the tensile strength depends on %fiberglass. Similarly, the non-parallel lines in the interaction plot of printing speed and %fiberglass show that the effect of printing speed on the tensile strength depends on %fiberglass.

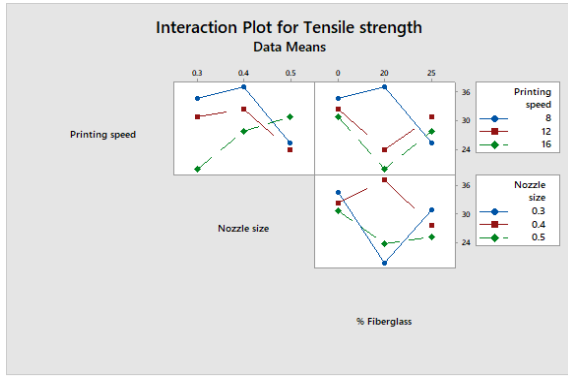

Figure 8: Interaction plot for tensile strength.

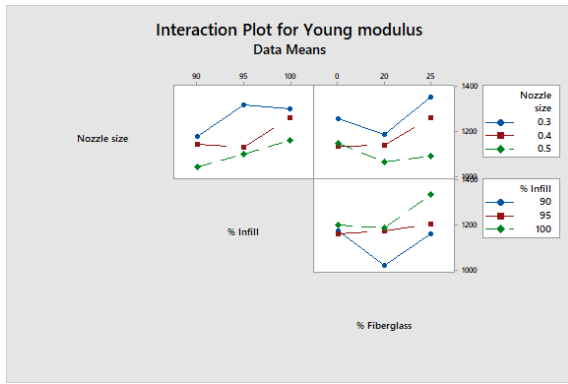

Figure 9: Interaction plot for Young's modulus.

Figure 9 presents the interaction plot of nozzle size, %infill, and %fiberglass with effect on Young's modulus. The non-parallel lines in the interaction plot of nozzle size and %infill show that the effect of nozzle size on Young's modulus depends on %infill.

Table 4: ANOVA for tensile strength

Source	DF	Adj SS	Adj MS	F-Value
% Fiberglass	2	110.60	55.30	1.48
Printing temperature	2	82.94	41.47	1.11
Printing speed	2	118.43	59.22	1.59
Nozzle size	2	106.32	53.16	1.42
% Infill	2	16.02	8.01	0.21
Heat bed Temperature	2	0.76	0.38	0.01

R^2 = 69.97%

Table 5: ANOVA for Young's modulus

Source	DF	Adj SS	Adj MS	F-Value
% Fiberglass	2	33814	16907	2.2
Printing temperature	2	6124	3062	0.4
Printing speed	2	4253	2126	0.28
Nozzle size	2	82535	41268	5.37
% Infill	2	43699	21850	2.84
Heat bed Temperature	2	3041	1520	0.2

$R^2 = 81.87\%$

Tables 4 and 5 show the two-way ANOVA for tensile strength and Young's modulus. The results indicated that printing speed, %fiberglass, and nozzle size are the top 3 parameters that affect tensile strength. The nozzle size, %infill and %fiberglass are the top 3 parameters that affect Young's modulus. In summary, the results of ANOVA are similar to the result of the main effect plot.

4 Conclusions

This study succeeded in developing the screw-based material extrusion 3D printing machine which can completely print the specimens from pellets of ABS and fiberglass/ABS composites. There were six studied process parameters: 1) the mixing ratio between fiber and ABS (% fiberglass), 2) the nozzle's temperature (printing temperature), 3) the speed of the nozzle movement (printing speed), 4) the bore size of the nozzle (nozzle size), 5) the percentage of the material infill in the 3D printing process (% infill), and 6) heat bed temperature. The printing speed, nozzle size, and %fiberglass are the top 3 parameters that affect tensile strength. It was found that the nozzle size, %infill, and %fiberglass are the top 3 parameters that affect Young's modulus. The optimum process parameters of neat ABS for tensile strength are %fiberglass = 0%, printing temperature = 205 °C, printing speed = 10 mm/s, nozzle size = 0.4 mm, %infill =100%, heat bed temperature = 70 °C. The optimum process parameters of glass/fiber ABS composite for Young's modulus are %fiberglass = 25%, printing temperature = 210 °C, printing speed = 18 mm/s, nozzle size = 0.3 mm, %infill =100%, heat bed temperature = 70 °C. The limitation of screw-based material extrusion 3D printing machine is the difficulty in controlling the consistency of extruded plastic line from the extruder resulting small gap between layers and reducing properties. The future work plans to develop feedback control to completely control the process parameters of screw-extruder speed and temperature.

Acknowledgments

This research was funded by Science and Technology Research Institute, King Mongkut's University of Technology North Bangkok THAILAND with contract no. KMUTNB-66-BASIC-10.

Author Contributions

T.S.: research design, investigation, methodology, data analysis, writing an original draft, writing reviewing and editing. L.T.: conceptualization, data analysis, writing reviewing and editing. All authors have read and agreed to the published version of the manuscript.

Conflicts of Interest

The authors declare no conflict of interest.

References

[1] M. Pant, R. M. Singari, P. K. Arora, G. Moona, and H. Kumar, "Wear assessment of 3-D printed parts of PLA (polylactic acid) using Taguchi design and Artificial Neural Network (ANN) technique," *Materials Research Express*, vol. 7, Nov. 2020, Art. no. 115307.

[2] R. Teharia, G. Kaur, and M. J. Akhtar, "Impact of additive manufacturing in value creation methods Applications and Challenges," in *ICAPIE 2019*, 2021, pp. 543–554.

[3] B. Devarajan, R. L. Narasimhan, B. Venkateswaran, S. M. Rangappa, and S. Siengchin, "Additive manufacturing of jute fiber reinforced polymer composites: A concise review of material forms and methods," *Polymer Composites*, vol. 43, pp. 6735–6748, Jun. 2022, doi:10.1002/pc.26789.

[4] M. Priyadharshini, D. Balaji, V. Bhuvaneswari, L. Rajeshkumar, S. M. Rangappa, and S. Siengchin, "Fiber reinforced composite manufacturing with the aid of artificial intelligence – A state-of-the-art review," *Archives of Computational Methods in Engineering*, vol. 29, pp. 5511–5524, Jun. 2022, doi: 10.1007/s11831-022-09775-y.

[5] Q. Yan, H. Dong, J. Su, J. Han, B. Song, Q. Wei, and Y. Shi, "A review of 3D printing technology for medical applications," *Engineering*, vol. 4, pp. 729–742, Oct. 2018, doi: 10.1016/j.eng.2018.07.021.

[6] P. Tack, J. Victor, P. Gemmel, and A. Lieven, "3D-printing techniques in a medical setting: A systematic literature review," *BioMedical Engineering OnLine*, vol. 15, Oct. 2016, Art. no. 115.

[7] S. Wang, X. Chen, X. Han, X. Hong, X. Li, H. Zhang, M. Li, Z. Wang, and A. Zheng, "A review of 3D printing technology in pharmaceutics: Technology and applications, now and future," *Pharmaceutics*, vol. 15, Jan. 2023, Art. no. 416.

[8] S. Kuntanapreeda and D. Hess, "Opening access to space by maximizing utilization of 3D printing in launch vehicle design and production," *Applied Science and Engineering Progress*, vol. 14, pp. 143–145, Jun. 2021, doi: 10.14416/j.asep.2020.12.002.

[9] A. Aslan and Y. Celik, "A literature review on 3D printing technologies in education," *International Journal of 3D Printing Technologies and Digital Industry*, vol. 6, pp. 592–613, Dec. 2022, doi: 10.46519/ij3dptdi.1137028.

[10] A. Jandyal, I. Chaturvedi, I. Wazir, A. Raina, and M. U. Haq, "3D printing – A review of processes, materials and applications in industry 4.0," *Sustainable Operations and Computers*, vol. 3, pp. 33–42, Oct. 2021, doi: 10.1016/j.susoc.2021.09.004.

[11] S. Singh, G. Singh, C. Prakash, and S. Ramakrishna, "Current status and future directions of fused filament fabrication," *Journal of Manufacturing Processes*, vol. 55, pp. 288–306, Apr. 2020, doi: 10.1016/j.jmapro.2020. 04.049.

[12] E. G. Gordeev, A. S. Galushko, and V. P. Ananikov, "Improvement of quality of 3D printed objects by elimination of microscopic structural defects in fused deposition modeling," *PLoS One*, vol. 13, Jun. 2018, Art. no. e0198370.

[13] C. Hu and Q. H. Qin, "Advances in fused deposition modeling of discontinuous fiber/polymer composites," *Current Opinion in Solid State and Materials Science*, vol. 24, Oct. 2020, Art. no. 100867.

[14] J. W. Choi, F. Medina, C. Kim, D. Espalin, D. Rodriguez, B. Stucker, and R. Wicker, "Development of a mobile fused deposition modeling system with enhanced manufacturing flexibility," *Journal of Materials Processing Technology*, vol. 211, pp. 424–432, Mar. 2011, doi: 10.1016/j.jmatprotec.2010.10.019.

[15] J. Mireles, H. C. Kim, I. H. Lee, D. Espalin, F. Medina, E. MacDonald, and R. Wicker, "Development of a fused deposition modeling system for low melting temperature metal alloys," *Journal of Electronic Packaging*, vol. 135, Mar. 2013, Art. no. 011008.

[16] W. C. Lee, C. C. Wei, and S. C. Chung, "Development of a hybrid rapid prototyping system using low-cost fused deposition modeling and five-axis machining," *Journal of Materials Processing Technology*, vol. 214, pp. 2366–2374, Nov. 2014, doi: 10.1016/ j.jmatprotec.2014.05.004.

[17] S. Maidin, J. H. U. Wong, A. S. Mohamed, and S. B. Mohamed, "Effect of vacuum assisted fused deposition modeling on 3D printed ABS microstructure," *International Journal of Applied Engineering Research*, vol. 12, pp. 4877–4881, Jan. 2017.

[18] S. Maidin, A. S. Mohamed, S. Akmal, S. B. Mohamed, and J. H. U. Wong, "Feasibility study of vacuum technology integrated fused deposition modeling to reduce staircase effect," *Journal of Fundamental and Applied Sciences*, vol. 10, pp. 633–645, Mar. 2018.

[19] E. S. Heras, F. B. Haro, J. M. D. A. del Burgo, M. I. Marcos, and R. D'Amato, "Filament advance detection sensor for fused deposition modelling 3D printers," *Sensors*, vol. 18, May 2018, Art. no. 1495.

[20] A. M. Al-Ahmari, O. Abdulhameed, and A. A. Khan, "An automatic and optimal selection of parts orientation in additive manufacturing," *Rapid Prototyping Journal*, vol. 24, pp. 698–708, May 2018, doi: 10.1108/RPJ-12-2016-0208.

[21] M. Ramesh, L. Rajeshkumar, and D. Balaji, "Influence of process parameters on the properties of additively manufactured fiber-reinforced polymer composite materials: A review," *Journal of Materials Engineering and Performance*, vol. 30, pp. 4792–4807, May 2021, doi: 10.1007/s11665-021-05832-y.

[22] A. Dogru, A. Sozen, G. Neser, and M. O. Seydibeyoglu, "Effects of aging and infill pattern on mechanical

properties of hemp reinforced PLA composite produced by fused filament fabrication (FFF)," *Applied Science and Engineering Progress*, vol. 14, pp. 651–660, Aug. 2021, doi: 10.14416/j.asep. 2021.08.007.

[23] C. Abeykoon, P. Sri-Amphorn, and A Fernando, "Optimization of fused deposition modeling parameters for improved PLA and ABS 3D printed structures," *International Journal of Lightweight Materials and Manufacture*, vol. 3, pp. 284–297, May 2020, doi: 10.1016/j.ijlmm. 2020.03.003.

[24] M. Kamaal, M. Anas, H. Rastogi, N. Bhardwaj, and A. Rahaman, "Effect of FDM process parameters on mechanical properties of 3D-printed carbon fibre-PLA composite," *Progress in Additive Manufacturing*, vol. 6, pp. 63–69, Feb. 2021, doi: 10.1007/s40964-020-00145-3.

[25] R. Omer, H. S. Mali, and S. K. Singh, "Tensile performance of additively manufactured short carbon fibre-PLA composites: Neural networking and GA for prediction and optimization," *Plastics, Rubber and Composites*, vol. 49, pp. 271–280, Mar. 2020, doi: 10.1080/14658011. 2020.1744371.

[26] V. D. P. Rao, P. Rajiv, and V. N. Geethika, "Effect of fused deposition modelling (FDM) process parameters on tensile strength of carbon fibre PLA," *Materials Today: Proceedings*, vol. 18, pp. 2012–2018, Nov. 2019, doi: 10.1016/j.matpr. 2019.06.009.

[27] Y. Y. Lim, A. Miskon, A. M. A. Zaidi, M. M. H. M. Ahmad, and M. A. Bakar, "Structural characterization analyses of low brass filler biomaterial for hard tissue implanted scaffold applications," *Materials*, vol. 15, Feb. 2022, Art. no. 1421.

[28] Y. Y. Lim, A. Miskon, and A. M. A. Zaidi, "Structural strength analyses for low brass filler biomaterial with anti-trauma effects in articular cartilage scaffold design," *Materials*, vol. 15, Jun. 2022, Art. no. 4446.

[29] Y. Y. Lim, A. Miskon, and A. M. A. Zaidi, "CuZn complex used in electrical biosensors for drug delivery systems," *Materials*, vol. 15, Nov. 2022, Art. no. 7672.

[30] Y. Y. Lim, A. M. A. Zaidi, and A. Miskon, "Combining copper and zinc into a biosensor for anti-chemoresistance and achieving osteosarcoma therapeutic efficacy," *Molecules*, vol. 28, Mar. 2023, Art. no. 2920.

[31] *Standard test method for tensile properties of plastics*, ASTM Standard D638−14, 2022.

[32] N. Kumar, P. K. Jain, P. Tandon, and P. M. Pandey, "Extrusion-based additive manufacturing process for producing flexible parts," *Journal of the Brazilian Society of Mechanical Sciences and Engineering*, vol. 40, Feb. 2018, Art. no. 143.

[33] N. Kumar, P. K. Jain, P. Tandon, and P. M. Pandey, "Experimental investigations on suitability of polypropylene (PP) and ethylene vinyl acetate (EVA) in additive manufacturing," *Materials Today: Proceedings*, vol. 5, pp. 4118–4127, Mar. 2018, doi: 10.1016/j.matpr.2017. 11.672.

[34] D. Jiang and D. E. Smith, "Anisotropic mechanical properties of oriented carbon fiber filled polymer composites produced with fused filament fabrication," *Additive Manufacturing*, vol. 18, pp. 84–94, Dec. 2017, doi: 10.1016/j.addma. 2017. 08.006.

[35] R. Teharia, R. M. Singari, and H. Kumar, "Optimization of process variables for additive manufactured PLA based tensile specimen using taguchi design and artificial neural network (ANN) technique," *Materials Today: Proceedings*, vol. 56, pp. 3426–3432, Apr. 2022, doi: 10.1016/ j.matpr.2021.10.376.